

# Journal of Mechanics of Materials and Structures

**ELASTIC BUCKLING CAPACITY OF BONDED AND UNBONDED  
SANDWICH PIPES UNDER EXTERNAL HYDROSTATIC PRESSURE**

Kaveh Arjomandi and Farid Taheri

**Volume 5, No. 3**

**March 2010**

## ELASTIC BUCKLING CAPACITY OF BONDED AND UNBONDED SANDWICH PIPES UNDER EXTERNAL HYDROSTATIC PRESSURE

KAVEH ARJOMANDI AND FARID TAHERI

Sandwich pipes can be a potentially optimal system for use in deep-water applications. In recent years, there has been considerable interest in understanding the stability characteristics of these pipes under the governing loading conditions, with the aim of generating optimal design. External hydrostatic pressure is a critical loading condition that a submerged pipeline experiences during its installation and operational period.

This article presents an analytical approach for estimating the buckling capacity of sandwich pipes with various structural configurations and core materials, subject to external hydrostatic pressure. The influence of adhesion between the core layer and inner or outer pipes is also a focus of this study. Beside the exact solution, two simplified equations are developed for estimating the buckling capacity of two configurations commonly used in practice. Details of both the exact and simplified analytical formulations are presented and the required parameters are defined. The efficiency and integrity of the proposed simplified solutions are compared with a solution developed by other researchers. A comprehensive series of finite element eigenvalue buckling analyses was also conducted to evaluate the accuracy and applicability of the proposed solutions.

*A list of symbols can be found on page 407.*

### Introduction

As shallow offshore oil reserves are depleted, the demand for deep water oil reserves is increasing. Extracting oil from deep waters will not be possible, unless new pipeline systems can be developed to accommodate the new loading and environmental conditions. High external hydrostatic pressure, pipeline buoyancy during installation, and low water temperatures restrict the application of single metallic pipelines to a limited depth. Sandwich pipes can be a potentially optimal design alternative in addressing the requirements of deep waters. Sandwich pipe (SP) systems employ the structural and thermal insulation benefits provided by two stiffer pipes sandwiching a lighter-weight and less stiff core material. Moreover, the secondary containment provided by the outer pipe improves the reliability of the system in the case of product leak.

A typical pipe in pipe (PIP) system consists of an inner pipe, a relatively thick lightweight core layer, and an outer pipe. Each layer in this system can be designed for a specific purpose. The inner pipe, also referred to as the product pipe, usually is designed to endure the internal pressure and to facilitate the transport of the product safely. The core layer's function can be different depending on the application. For example, it can be designed to act as a thermal insulator, or to improve the structural performance of the pipeline, depending on the core's material properties and the interaction mechanism between the

---

*Keywords:* sandwich pipes, pipe-in-pipe, stability, buckling, hydrostatic pressure.

core layer and the surrounding pipes. A wide range of core materials such as plastics, gels, ceramics, and composites can be used to achieve the system's thermal and structural requirements. The outer pipe, also called the sleeve pipe, separates the inner and core layers from the surrounding environment. The sleeve pipe may individually carry the externally applied loads, as in a PIP system, or may act as the main part of a sandwich system, as in an SP system. The outer pipe also provides secondary containment for the product being transported, in case of leakage of the product through the inner pipe.

To design an optimal SP system, understanding of its structural behavior is a prerequisite. A great number of works have been written in recent years to clarify the structural characteristics of such a system under different loading conditions. Some of those works have considered the stability of a sandwich cylindrical shell, which can be a general geometry for a sandwich pipe. For example Kyriakides and his coworkers studied buckle propagation phenomena [Kyriakides 2002; Kyriakides and Netto 2002; 2004; Kyriakides and Vogler 2002] from both numerical and experimental perspectives. Kardomateas and Simitse [2002; 2005] studied analytically the buckling of long sandwich cylindrical shells under external pressure. Ohga et al. [2005] studied, both numerically and analytically, the reduced stiffness buckling of sandwich cylindrical shells under uniform external pressure. Sato and Patel [2007] and Sato et al. [2008] studied the buckling behavior of a PIP system under hydrostatic pressure and developed a simplified solution for estimating a PIP system's buckling capacity. Castello and Estefen [2006; 2008] and Estefen et al. [2005] studied the feasibility of a sandwich pipe system for deep water applications with both numerical and experimental approaches. In another study, Castello and Estefen [2007] investigated the ultimate strength of sandwich pipes under combined external pressure and bending for several degrees of adhesion between the core layer and outer pipe. They also investigated the effect of cyclic loads applied during a reeling installation on the collapse pressure. Very recently, Castello et al. [2009] also conducted an investigation, comparing PIP and SP systems designed for a hypothetical oil field with several core materials. In this study they used polypropylene and polyurethane foams with various densities as the core materials and investigated the influences of both their mechanical and thermal properties. They concluded that the combination of steel and foams could produce effective SP systems with good buoyancy and thermal insulation properties.

## 1. Motivation and aims

Our preliminary investigation indicated that most of the available simplified solutions developed for predicting buckling capacity of PIP systems subject to hydrostatic pressure produce results with very large margins of error under certain conditions. This fact prompted an analytical investigation, with the aim of developing exact and simplified solutions for establishing the buckling capacity of PIPs subject to externally applied hydrostatic pressure. Moreover, a comprehensive finite element investigation is also conducted to establish the performance of PIPs with a wide range of material and physical properties, and to verify the integrity of the proposed solutions. Four different interlayer bonding configurations are considered. The parameters used to define the characteristic equation of the system are outlined. An important aim of this investigation is also extracting simplified solutions from the exact solution for use in practical design. As a result, the simplified and exact solutions are compared and the accuracy of their results discussed. Finally, the error margins resulting from the use of the proposed simplified equations and those resulting from the proposals of other researchers are established.

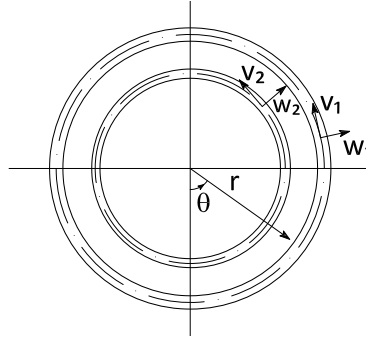


**Figure 1.** The coordinate system and the idealized geometry.

## 2. The analytical model

A long, circular cylindrical shell with three layers (steel, core, and steel) is considered. Due to the symmetry in structural configuration and loading, this problem can be idealized as a two-dimensional plane strain problem. The use of polar coordinates also aids in the formulation the problem. [Figure 1](#) shows the geometry and polar coordinate system of the model.

**Equilibrium equations of the system.** The potential energy of the system can be used to derive the equilibrium equations. It can be represented as follows [[Kyriakides and Corona 2007](#)]:

$$\Pi = U_{P,1} + U_{P,2} + U_c + W_p, \quad (1)$$

where the potential energies of the inner and outer pipes are given by

$$U_{P,i} = \int_0^{2\pi} \frac{1}{2} [N_{\theta\theta,i} \varepsilon_{\theta\theta,i}^o + M_{\theta\theta,i} k_{\theta\theta,i}] r_i \cdot d\theta, \quad (2)$$

where  $i = 1$  for the outer pipes and  $i = 2$  for the inner one,  $N_{\theta\theta}$  is the internal axial force,  $\varepsilon_{\theta\theta}^o$  is the circumferential strain of the centroid fiber,  $M_{\theta\theta}$  is the internal moment, and  $k_{\theta\theta}$  is the curvature change in the centroid surface.

In (1), the effect of the core layer can be considered as the work done by the entire layer's stresses applied to the inner and outer pipes. These works can be represented by

$$U_c = U_{c,1} + U_{c,2}, \quad \text{where} \quad U_{c,i} = \int_0^{2\pi} (\sigma_r|_{a_i} \cdot w|_{a_i} + \tau_{r\theta}|_{a_i} \cdot v|_{a_i}) a_i \cdot d\theta, \quad (3)$$

where  $a_1 = r_1 - t_1/2$  and  $a_2 = r_2 + t_2/2$ .

The work done by the external hydrostatic pressure is given by

$$W_P = P \int_0^{2\pi} (wr_1 + \frac{1}{2}(v^2 + w^2 - vw' + v'w)) \cdot d\theta, \quad (4)$$

where the  $'$  indicates the differentiation with respect to  $\theta$ .

Sander's shell equations are used to describe the strain-displacement relationships. Sander's kinematic equations are nonlinear and are based on small strain and moderate rotation assumptions, which are appropriate for establishing the linear buckling equations. The kinematic equations in polar coordinate

can be written as

$$\varepsilon_{\theta\theta} = \varepsilon_{\theta\theta}^o + z k_{\theta\theta}, \quad \varepsilon_{\theta\theta}^o = \frac{w+v'}{r} + \frac{1}{2}\beta^2, \quad k_{\theta\theta} = \frac{\beta'}{r}. \quad (5)$$

In these equations  $\beta$  represents the rotation of a circumferential element located at the midplane of the pipes.  $\beta$  for an intermediate class of deformation (small midsurface strains and small but finite rotations) can be defined as in [Farshad 1994] by as

$$\beta = \frac{v-w'}{r}. \quad (6)$$

Using the plane strain material constitutive relation, we get for the force and moment intensities in (2)

$$N_{\theta\theta} = C\varepsilon_{\theta\theta}^o, \quad M_{\theta\theta} = Dk_{\theta\theta}, \quad (7)$$

where  $C = Et/(1 - \nu_p^2)$  and  $D = \frac{1}{12}Et^3/(1 - \nu_p^2)$ .

By substituting the kinematic and constitutive equations and using variational calculus, we can write the equilibrium equations of the system as

$$\alpha_{1,1}(w_1 + v_1') - \alpha_{2,1}(v_1 - w_1')''' + p(w_1'' + w_1) + a_1\sigma_r|_{a_1} = 0, \quad (8a)$$

$$\alpha_{1,1}(w_1 + v_1')' + \alpha_{2,1}(v_1 - w_1')'' + a_1\tau_{r\theta}|_{a_1} = 0, \quad (8b)$$

$$\alpha_{1,2}(w_1 + v_1') - \alpha_{2,2}(v_1 - w_1')''' - a_2\sigma_r|_{a_2} = 0, \quad (8c)$$

$$\alpha_{1,2}(w_1 + v_1')' + \alpha_{2,2}(v_1 - w_1')'' - a_2\tau_{r\theta}|_{a_2} = 0, \quad (8d)$$

where

$$\alpha_{1,i} = \frac{C_i}{r_i}, \quad \alpha_{2,i} = \frac{D_i}{r_i^3} \quad (i = 1, 2). \quad (8e)$$

These Euler differential equations are written in terms of the four independent variables  $u_1$ ,  $v_1$ ,  $u_2$ , and  $v_2$ , which represent the deformation of the inner and outer pipes, and four dependent variables  $\sigma_r|_{a_1}$ ,  $\tau_{r\theta}|_{a_1}$ ,  $\sigma_r|_{a_2}$ , and  $\tau_{r\theta}|_{a_2}$ . The dependent variables can be described as functions of the independent variables, using the core properties. An elasticity approach is used here to characterize the core behavior.

The displacement function that could satisfy the equilibrium equations can be assumed to be circumferentially periodic. Considering this assumption, the following stress function would satisfy the equilibrium equations [Sato and Patel 2007]:

$$\phi(r, \theta) = f_n(r) \cos n\theta, \quad (9)$$

where  $n$  is the buckling mode number. To yield a possible stress distribution, the stress function must be such that the following compatibility equation is satisfied [Timoshenko and Goodier 1970]:

$$\left( \frac{\partial^2}{\partial r^2} + \frac{1}{r} \frac{\partial}{\partial r} + \frac{1}{r^2} \frac{\partial^2}{\partial \theta^2} \right) \left( \frac{\partial^2 \phi}{\partial r^2} + \frac{1}{r} \frac{\partial \phi}{\partial r} + \frac{1}{r^2} \frac{\partial^2 \phi}{\partial \theta^2} \right) = 0. \quad (10)$$

In order for  $\phi$  to be an admissible solution of this equation, the general form of  $f_n$  must be as follows [Timoshenko and Goodier 1970]:

$$f_n(r) = A_n r^{-n} + B_n r^{2-n} + C_n r^{2+n} + D_n r^n \quad (n \geq 2), \quad (11)$$

in which the constants  $A_n$ ,  $B_n$ ,  $C_n$ , and  $D_n$  are calculated from the distribution of forces and displacements at the boundaries. The stress and displacement components in polar coordinates are

$$\sigma_r = \frac{1}{r} \frac{\partial \phi(r, \theta)}{\partial r} + \frac{1}{r^2} \frac{\partial^2 \phi(r, \theta)}{\partial \theta^2}, \quad \tau_{r\theta} = -\frac{\partial}{\partial r} \left( \frac{1}{r} \frac{\partial \phi(r, \theta)}{\partial \theta} \right), \quad \tilde{w} = \int \varepsilon_r \cdot dr, \quad \tilde{v} = \int (r\varepsilon_\theta - w) \cdot d\theta. \quad (12)$$

Using these relations, stresses at the boundary of the core can be described as a function of the deformation of the boundary. The following general core boundary conditions are considered:

$$\tilde{w}|_{a_1} = \tilde{W}_1 \cos n\theta, \quad \tilde{v}|_{a_1} = \tilde{V}_1 \sin n\theta, \quad \tau_{r\theta}|_{a_1} = 0, \quad (13)$$

$$\tilde{w}|_{a_2} = \tilde{W}_2 \cos n\theta, \quad \tilde{v}|_{a_2} = \tilde{V}_2 \sin n\theta, \quad \tau_{r\theta}|_{a_2} = 0. \quad (14)$$

Four sets of boundary conditions are chosen depending on the problem:

- I. Core is fully bonded to both inner and outer pipes: boundary conditions (13)<sub>1,2</sub> and (14)<sub>1,2</sub>.
- II. Core is unbonded to the outer pipe in the tangential direction, but is fully bonded to the inner pipe: boundary conditions (13)<sub>1,3</sub> and (14)<sub>1,2</sub>.
- III. Core is unbonded to the inner pipe in the tangential direction, but is fully bonded to the outer pipe: boundary conditions (13)<sub>1,2</sub> and (14)<sub>1,3</sub>.
- IV. Core can slide freely against both inner and outer pipes: boundary conditions (13)<sub>1,3</sub> and (14)<sub>1,3</sub>.

**Characteristic equation of the system.** We denote the stiffness matrices of the pipes and core by  $K_p = [p_{ij}]_{0 \leq i, j \leq 4}$  and  $K_c = [c_{ij}]_{0 \leq i, j \leq 4}$ . The nonzero coefficients of  $K_p$  are

$$p_{11} = \alpha_1 \left[ 1 + \frac{1}{12} \left( \frac{t_1}{r_1} \right)^2 n^4 \right] + q(n^2 - 1), \quad p_{22} = \alpha_1 n^2 \left[ -1 + \frac{1}{12} \left( \frac{t_1}{r_1} \right)^2 \right], \quad p_{12} = -p_{21} = \alpha_1 n \left[ 1 + \frac{1}{12} \left( \frac{t_1}{r_1} \right)^2 n^2 \right],$$

$$p_{33} = \alpha_2 \left[ 1 + \frac{1}{12} \left( \frac{t_2}{r_2} \right)^2 n^4 \right], \quad p_{44} = \alpha_2 n^2 \left[ -1 + \frac{1}{12} \left( \frac{t_2}{r_2} \right)^2 \right], \quad p_{34} = -p_{43} = \alpha_2 n \left[ 1 + \frac{1}{12} \left( \frac{t_2}{r_2} \right)^2 n^2 \right],$$

where

$$a_1 = r_1 - \frac{t_1}{2}, \quad a_2 = r_2 + \frac{t_2}{2}, \quad \alpha_1 = \frac{E_p t_1}{r_1 (1 - \nu_p^2)}, \quad \alpha_2 = \frac{E_p t_2}{r_2 (1 - \nu_p^2)}.$$

The coefficients of  $K_c$  are more complex and are given in the [Appendix](#).

The characteristic equation of the system can be written as

$$[K_p + K_c]\{\delta\} = 0, \quad (15)$$

where  $\delta$  represents the deformation of the structure in the form of a vector representing the radial and circumferential deformations of the inner and outer pipes. To obtain a nontrivial solution, the determinant of the coefficient matrix must be set to zero. By solving this eigenvalue equation, the buckling pressure of the sandwich pipe is determined.

The characteristic equation of a sandwich pipe is more complex than that of a single pipe. Because of this complexity, the mode number that yields the lowest buckling pressure is not necessarily 2. In the system under investigation, the first buckling mode ( $n = 1$ ) corresponds to a rigid body motion; therefore the characteristic equation must be solved for higher buckling modes.

### 3. Simplified solutions

A simplified solution was developed independently by [Brush and Almroth \[1975\]](#) and [Sato and Patel \[2007\]](#) for calculating the buckling pressure of a sandwich pipe under externally applied hydrostatic pressure; hereafter it is abbreviated as SS. The SS equation is

$$P_{cr} = P_{crs} + \frac{1}{n^2 - 1}k, \quad (16)$$

where

$$k = E_c \frac{2n(\nu_c - 1) - 2\nu_c + 1}{4\nu_c^2 + \nu_c - 3}, \quad P_{crs} = \left(\frac{t_1}{r_1}\right)^3 \frac{E_p(n^2 - 1)}{(1 - \nu_p^2)((t_1/r_1)^2 + 12)}.$$

This equation was developed by solving the buckling pressure of a ring supported internally by an elastic foundation. This would indicate that the continuity of the shear stresses between the core and outer pipe is ignored. Furthermore, the above equation was developed based on the assumption that the core can be replaced by a set of springs. The solution has been improved in this study by considering a proper stress function representing the core layer's response. In the mathematical model developed in this study, the continuity of the interlayer deformations and stresses was considered, and the characteristic equation of the system, which included the response of both core and pipes, was solved simultaneously.

In this section a set of simplified equations will be developed with the assumptions that  $r_2 \rightarrow 0$  and  $h_2 \rightarrow 0$ , indicating that the inner portion of the system (surrounded by the outer pipe) is filled entirely by the core material. It is indeed recognized that this assumption may not be entirely correct, violating the exact proportional equivalency of the inner steel pipe in terms of the core material; however, as will be seen later, this simplifying assumption facilitates the solution of an otherwise complex equation. Moreover, as will also be shown, the produced solution is capable of generating relatively accurate results.

The assumption above enables one to establish the buckling pressure of a sandwich pipe by satisfying the equation

$$\lim_{R \rightarrow 0} \lim_{h_2 \rightarrow 0} [K_p + K_c]\{\delta\} = 0. \quad (17)$$

The accuracy of the proposed simplified solution is discussed in the following sections.

**A: Core free to slide against outer pipe.** Using the simplifying assumptions above, the characteristic equation of the system was solved using Mathematica, leading to the following equation, which can be used to establish the critical buckling capacity (pressure) of a sandwich pipe whose core layer is unbonded from the outer pipe:

$$P_{cr} = P_{crs} + \frac{E_c}{[2n(1 - \nu_c) + 2\nu_c - 1](1 + \nu_c)}. \quad (18)$$

This satisfies (17), using boundary conditions [II](#) or [IV](#).

**B: Core bonded to outer pipe.** Using the same method, the following buckling pressure has been calculated by solving (17) with case [I](#) boundary conditions:

$$P_{cr} = \frac{\xi_1}{\xi_2}, \quad (19)$$

where

$$\begin{aligned} \xi_1 &= 192E_c^2 a_1 r_1^3 (v_p^2 - 1)^2 + E_p^2 t_1^4 n^2 \Lambda (n^2 - 1) (\Lambda + 7)^2 + 2E_c E_p r_1 t_1 (v_p^2 - 1) (\Lambda + 7) \\ &\quad \times \{t_1^2 n^2 [n(\Lambda - 1) - \Lambda - 1] - 6t_1 r_1 [(n + 1)^2 + (n - 1)^2 \Lambda] - 12r_1^2 [n(\Lambda - 1) - \Lambda - 1]\}, \\ \xi_2 &= r_1 (v_p^2 - 1) (\Lambda + 7) \{-12E_c r_1^2 a_1 (v_p^2 - 1) [n(\Lambda - 1) - \Lambda - 1] + E_p t_1 n^2 \Lambda (t_1^2 + 12r_1^2) (\Lambda + 7)\}. \end{aligned}$$

Here

$$\Lambda = 4\nu_c - 3. \quad (20)$$

For brevity, the simplified solutions just developed will be referred to as the ATS.

#### 4. Results and discussion

The histogram in [Figure 2](#) illustrates the number of standard and heavy wall line pipes available in the API standard [[API 2000](#)]. This histogram has been generated for API pipes with radii greater than 0.1 m, which is the most widely used range for offshore pipeline applications. As shown in this graph, the thickness to radius ratio in API pipe charts varies between 0.02 and 0.18.

**Exact solution results.** The ratio of the buckling pressure of an integral sandwich pipe to the buckling pressure of the outer pipe of a SP system can be written as a function of nondimensional parameters:

$$\frac{P_{cr}}{P_{crs}} = f\left(\frac{E_c}{E_p}, \frac{t_1}{r_1}, \nu_p, \nu_c, n\right), \quad (21)$$

where  $P_{crs}$  is the buckling pressure of the outer pipe; see the beginning of [Section 3](#). This ratio is used hereafter to present the results obtained from the proposed and SS solutions.

[Figure 3](#) shows the variation of the buckling pressure of a sandwich pipe with respect to the change in pipe geometry ( $r_2/r_1$ ) and pipe material properties ( $E_c/E_p$ ) in the aforementioned practical range. As stated, the buckling pressures of the sandwich pipes in these figures have been normalized with respect to that of the outer pipe. These graphs have been developed for a sandwich pipe with inner and outer pipe thickness to radius ratios of 0.05. In this study, Poisson's ratios of the core and pipes are taken as 0.5 and 0.3, respectively. As can be seen, the continuity of the shear stresses between the pipes and the core layer would significantly affect the buckling resistance of the pipe under external pressure. As

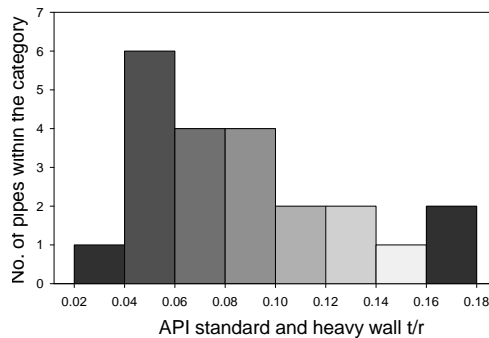


**Figure 2.** Histogram of  $t/r$  for API heavy and standard wall pipes with diameter greater than 0.1 m.

expected, the fully bonded configuration provides the greatest buckling capacity in comparison with the other configurations. The configuration in which the core layer and surrounding pipes are free to slide against each other exhibits the lowest buckling pressure. The difference between the buckling pressures of these two extreme configurations can be more than 100 times for certain values of  $r_2/r_1$  and  $E_c/E_p$ .

Figure 3, top left, shows that for the fully bonded case, the buckling pressure of sandwich pipes with wide ranges of  $r_2/r_1$  and  $E_c/E_p$  values is not significantly affected by the variation in the  $r_2/r_1$  parameter. This fact was used as the basis for driving the simplified equations based on the assumption that the equivalent structure would be a pipe (the outer pipe) filled with the core material. The same conclusion can be made by considering Figure 3, top right, for the lower range of  $r_2/r_1$ . As also seen, the buckling pressure in the other configurations is significantly dependent on the inner pipe diameter.

The other interesting results are associated with the pipe configuration in which the core and inner pipe can slide on one another. As can be seen in Figure 3, bottom left, there is no consistent trend for the buckling pressure within the studied range of parameters. By comparing the bottom left panes of Figures 3 and 5, which illustrate the buckling mode numbers for the same configuration, it can be concluded that the uneven behavior of the graph in the former is due to the oscillation in the buckling mode response of the pipe. Note that the actual buckling mode response of such sandwich pipes would not be exactly the same as what has been captured in our investigation. Indeed, the discrepancy between

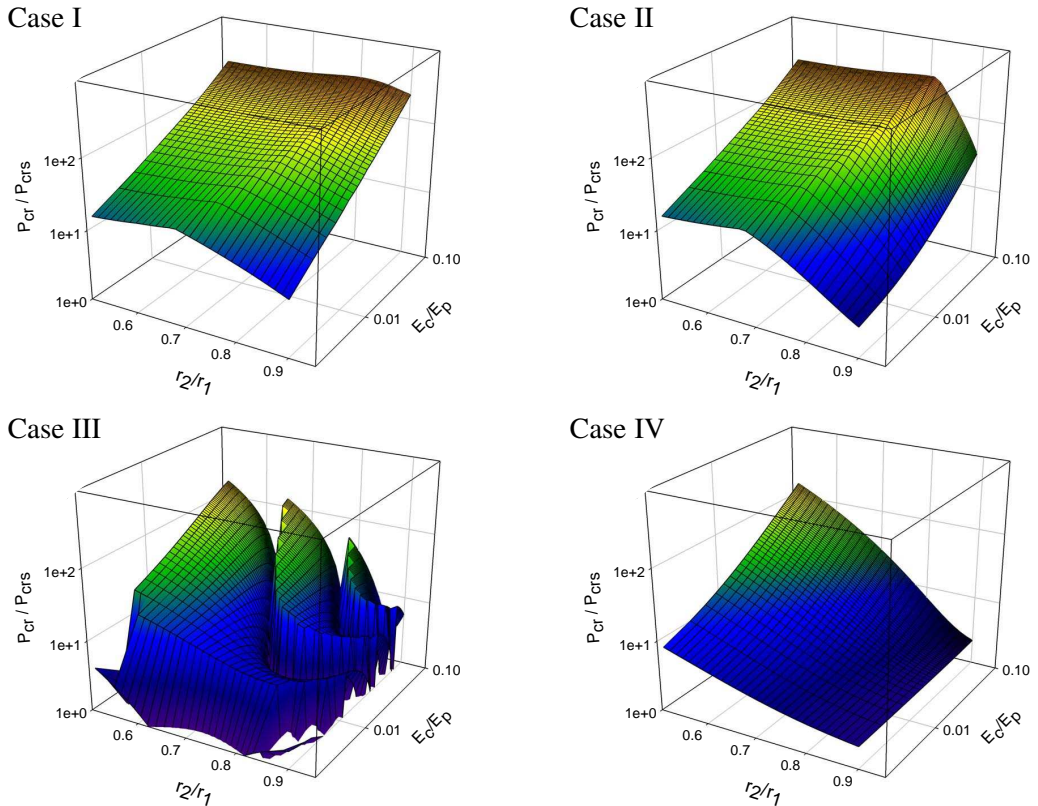


**Figure 3.** Ratio of buckling capacity of sandwich pipe versus outer pipe as a function of geometric and material properties for the cases discussed on page 395.

what has been considered as the general buckling mode shape in this study and what would happen in reality becomes more significant in sandwich pipes in which the core can freely slide on the inner pipe. This phenomenon is believed to be the cause the oscillation in the calculated buckling pressures corresponding to the different buckling mode shapes. For the sake of consistency, the logarithmic scale has been used in these figures, which magnifies the unevenness.

Figure 4 shows the variation of buckling pressure of the sandwich system as a function of the inner pipe's geometry ( $t_1/r_1$ ) and the pipeline material properties ( $E_c/E_p$ ) within the practical range. In these figures, the ratios  $r_2/r_1$  and  $t_2/r_2$  have been taken as 0.8 and 0.05, respectively. These graphs show that the buckling pressure of the system is significantly influenced by  $t_1/r_1$ . The bottom right graph in Figure 4 shows that if the core layer is free to slide on both the inner and outer pipes, then the increase in the core modulus of elasticity would not improve the structural performance of the pipe when subject to external pressure. For other configurations, however, the increase in the core's modulus of elasticity would increase the buckling pressure of the system.

According to the results exhibited in Figures 3 and 4, in order to design an optimal sandwich pipe under external hydrostatic pressure, close attention should be paid to the bonding properties between the layers, as well as the geometrical and material related parameters like  $E_c/E_p$ ,  $r_2/r_1$ , and  $t_1/r_1$ .

Figure 5 shows the mode number associated with the minimum buckling pressure of the SPs with various geometries and material properties. As illustrated in the figures, for the system under investigation,

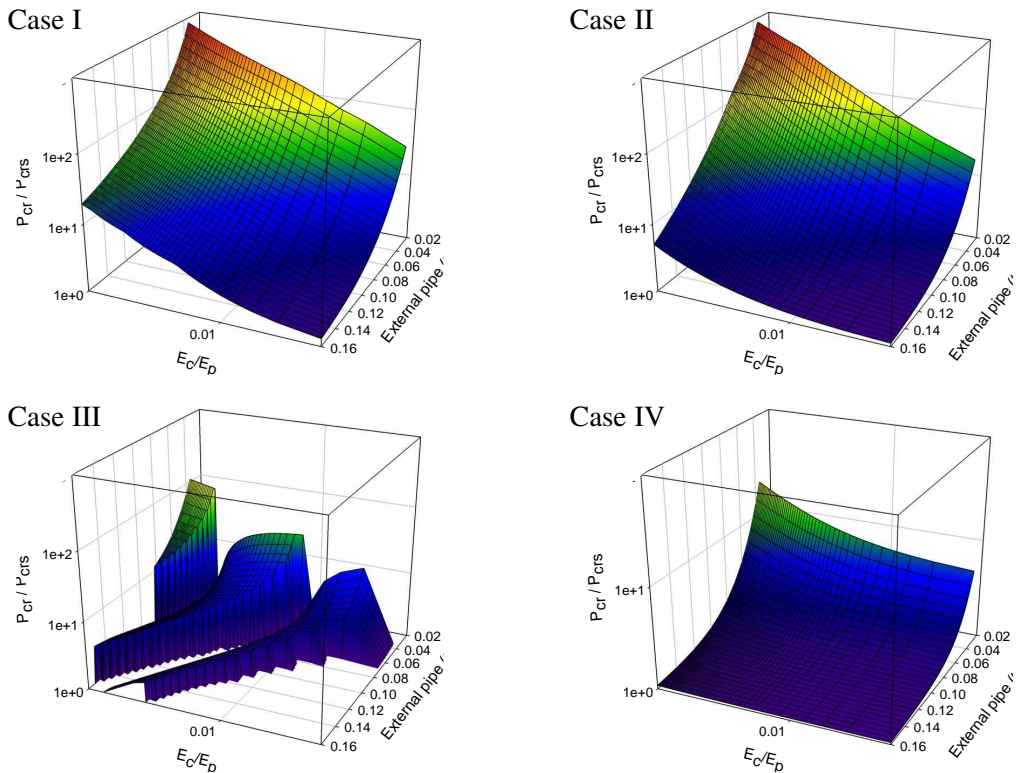


**Figure 4.** Ratio of buckling capacity of sandwich pipe to outer pipe as a function of geometric and material properties.

the buckling mode associated with the minimum buckling pressure of a sandwich pipe is not necessarily mode number 2. In fact, in most of the configurations studied, the buckling mode corresponding to the lowest capacity shifts upward as the core's stiffness is increased. The bottom right graph in [Figure 5](#) shows that for the fully unbonded case, the corresponding buckling mode number is mode number 2 for all the studied parameters ranges. This conclusion would help to simplify the calculations significantly.

**Accuracy of the simplified equations.** In this section, both simplified solutions (that is, both Sato and Patel's and our proposed solutions) are compared with the exact solution. The comparison is done for a sandwich system with core and pipe Poisson's ratios of 0.5 and 0.3, respectively. The percentage error is calculated by

$$\% \text{ error} = \left| \frac{P_{\text{cr}}(\text{Exact}) - P_{\text{cr}}(\text{Simplified})}{P_{\text{cr}}(\text{Exact})} \right| \times 100. \quad (22)$$

[Figure 6](#) shows the buckling pressure error in the SS solution, (16), relative to the exact values calculated by solving (15). This graph has been generated for case I boundary conditions (fully bonded case). As seen in the left half of the figure, this simplified equation would produce error up to 180% for the illustrated range of parameters. The right half reports the margin of error for a sandwich pipe with  $t_1/r_1 = 0.05$  and inner to outer pipe radius ratio of 0.8. We see that the error produced by (15) for the sample pipe is at least 120% and can be as large as 200%. In conclusion, the error produced by this equation increases as the core stiffness decreases and the outer pipe thickness to radius ratio increases.

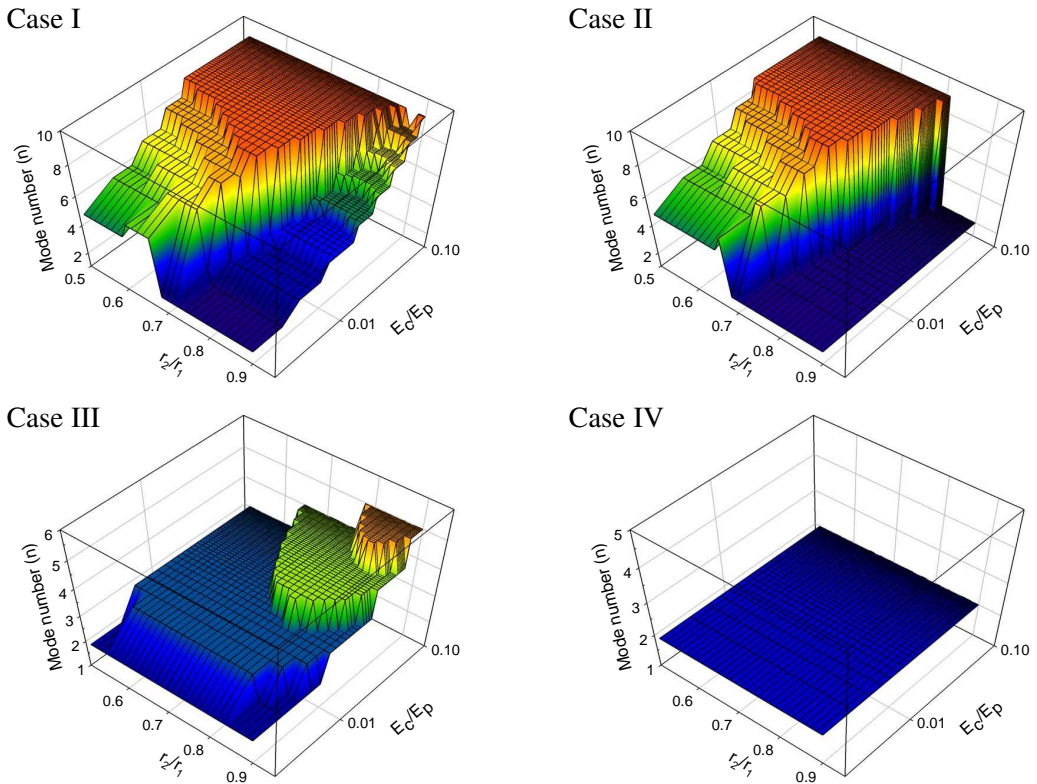


**Figure 5.** Sandwich pipe buckling mode numbers for the cases discussed on page 395.

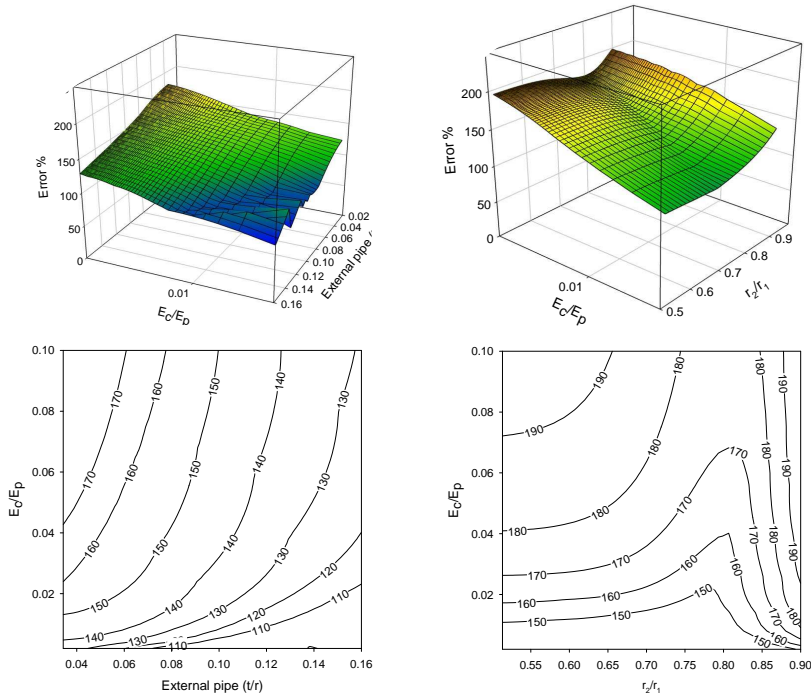


**Figure 6.** Percent error produced by the SS in the fully bonded case, as a function of  $E_c/E_p$  and the outer pipe's  $t/r$  ratio (left) and as a function of  $E_c/E_p$  and  $r_2/r_1$  (right).

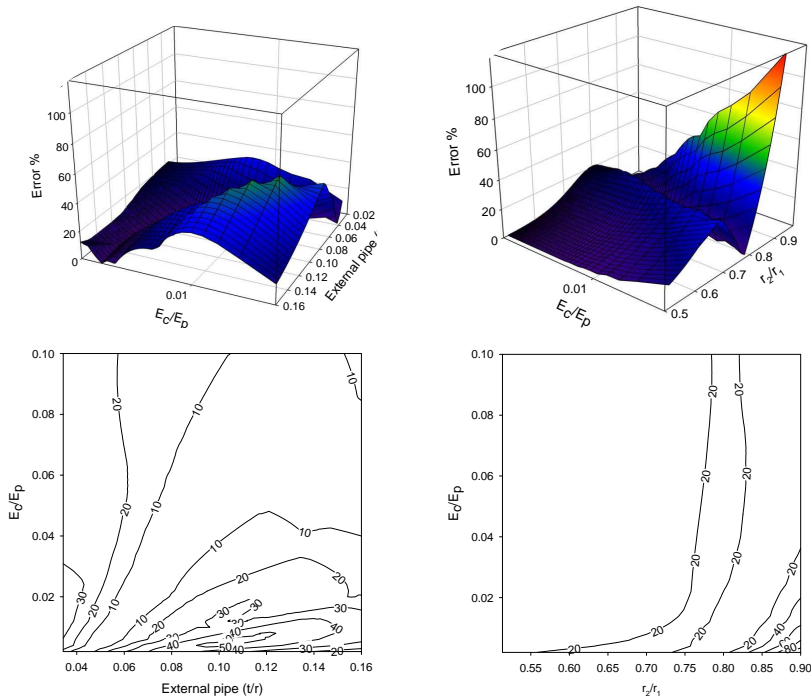


**Figure 7.** Percent error produced by the ATS in the fully bonded case, as a function of  $E_c/E_p$  and the outer pipe's  $t/r$  ratio (left) and as a function of  $E_c/E_p$  and  $r_2/r_1$  (right).

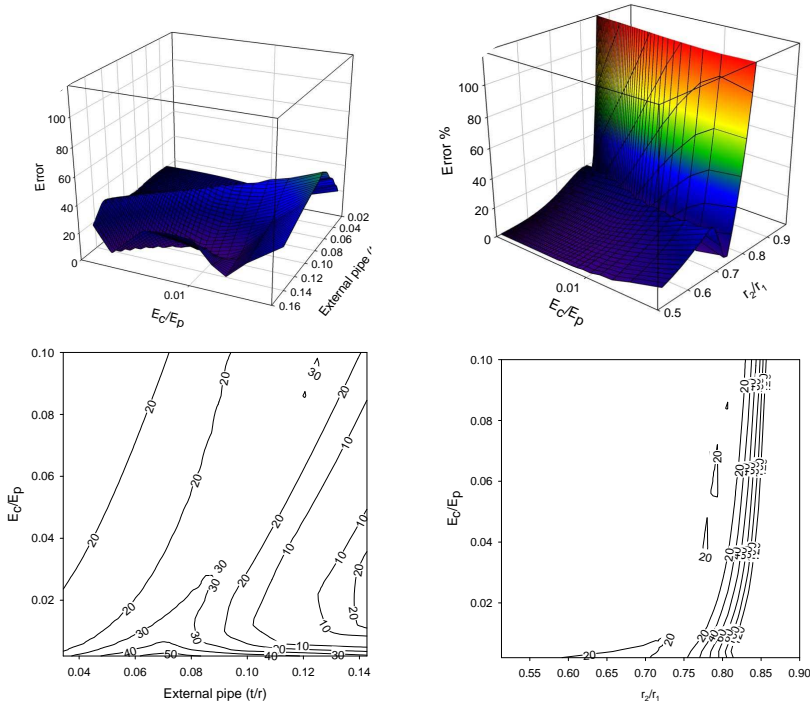


**Figure 8.** Percent error produced by the ATS for the case of the outer pipe sliding over the core, as a function of  $E_c/E_p$  and the outer pipe's  $t/r$  ratio (left) and as a function of  $E_c/E_p$  and  $r_2/r_1$  (right).

Figure 7 shows the percent error resulting from the ATS (19) (that is, the simplified solution developed in this study), for the case of a fully bonded SP. The figure suggests that the ATS yields more accurate results than the SS from (16). The SS produced a maximum error of 120%, where for the same pipe the ATS produces a maximum error of 50% in predicting the buckling pressure (in the worst possible case).

Figure 8 shows the percentage error produced by our simplified solution in predicting the buckling pressure of the pipe with core layer unbonded to the outer pipe. The exact results are obtained by solving (15), using type II boundary condition. As can be seen, the ATS produces very large errors for values of  $r_2/r_1$  above 0.75. However, if the inner to outer pipes radius ratio is below 0.75, the error is less than 20%. In practice, most PIP systems use  $r_2/r_1 < 0.75$ . Therefore, the ATS (19), would be admissible for use in practice. Figure 8, top right, shows the percent error for a sandwich pipe with a thickness to radius ratio of 0.05 and an inner to outer pipe radius ratio of 0.8.

### Numerical results

In this section a series of finite element (FE) eigenvalue analyses are performed for a parametric study to assess the accuracy of the proposed simplified solution. ABAQUS Version 6.8 was used to construct and analyze the FE models. Due to the assumption of uniform structural properties and loading conditions along the length of the pipeline, a sandwich ring was modeled as the equivalent structure, to study the buckling characteristic of the SP under hydrostatic pressure. The 20-node, reduced integration

brick element (C3D20R) was used to construct the finite element model of the pipes. In this paper, SP systems with incompressible core layers were investigated to establish the margin of error produced by the solutions outlined earlier. Therefore, the core layer was modeled with 20-node, reduced integration hybrid brick elements (C3D20RH), suited for modeling soft materials. Appropriate boundary conditions were applied to restrain the rigid body motions of the model; however, they were kept to a minimum so that the higher order buckling modes could be captured.

The “tie” multipoint constraint option of ABAQUS was used to model the fully bonded contacts between the core and inner and outer pipes. However, in those configurations in which the core layer was disbonded from the pipes, the contact mechanism was modeled using the linear two point constraint equations of ABAQUS. With this approach, the radial displacement of the core on the contact surfaces is set to follow the radial displacement of the contacting surfaces of the pipes, but no constraint is imposed on the tangential displacements. This approach is prone to error, because the elements may intersect. To minimize this possibility, a fine mesh must be used. A mesh convergence study was conducted to investigate the effect of the mesh density on the calculated buckling pressure. Figure 9 shows the buckling mode shapes of the four studied PIP configurations.

To test the integrity of the simplified solution, four sets of parametric studies were performed on the four analytically studied configurations. In each set, 1296 FE models were analyzed and the results were compared with those obtained using the simplified solution. Figure 10 shows the percent error produced by the simplified equations with respect to the FE results for the SS from (16), AST from (19), and AST from (18) cases.

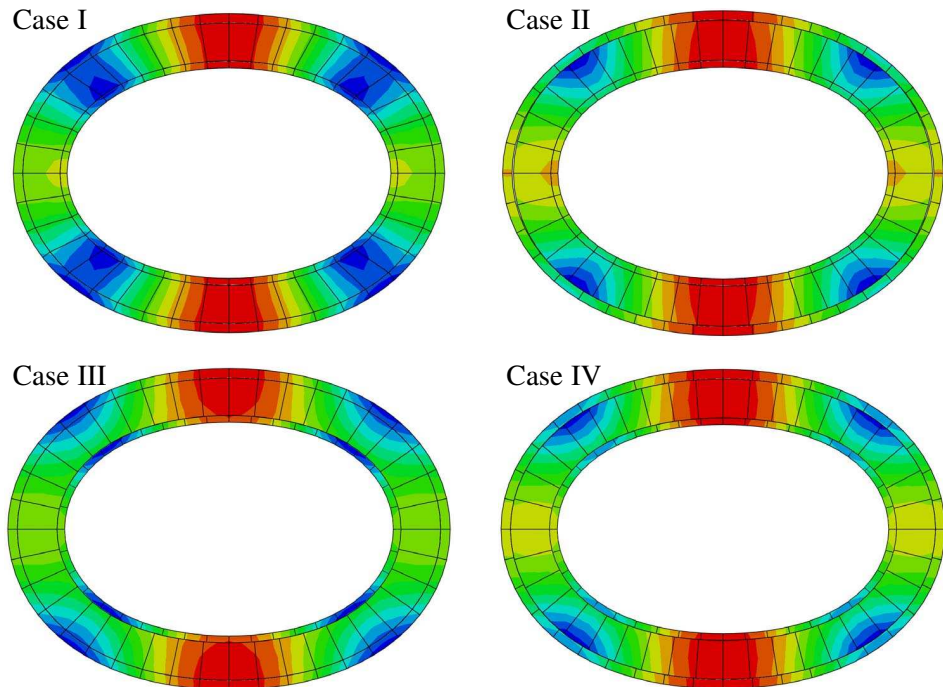


**Figure 9.** Buckling mode shapes for the cases discussed on page 395.

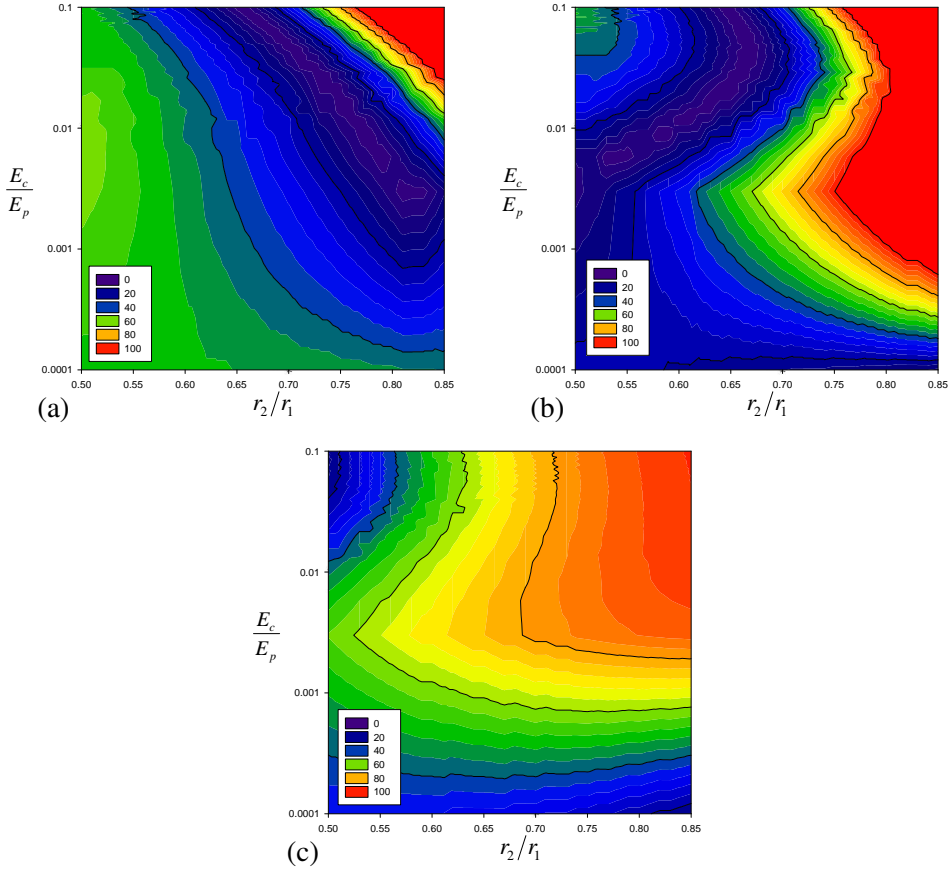


**Figure 10.** Percentage error produced by the simplified equations with respect to the FE results for (a) SS from (16), (b) AST from (19), and (c) AST from (18).

As shown in Figure 10a, the SS solution results in an error of less than 50% for larger values of  $r_2/r_1$ . The comparison of the results obtained by the ATS simplified from (19) and FE are illustrated in Figure 10b. As can be seen, the solution yields a maximum error of slightly less than 50% for smaller values of  $r_2/r_1$ . These graphs show that either solution can predict the buckling pressure of a sandwich pipe, for a limited range of the parameters, with reasonable accuracy.

Figure 10c shows the error margins when using (18) for a SP system in which the core layer is disbonded from the outer pipe. As illustrated in this figure, for  $E_c/E_p$  greater than  $10^{-3}$ , this equation yields an error of greater than 60%. However, for smaller values of  $E_c/E_p$ , which would pertain to most of the commonly used plastic materials, (18) would yield acceptable accuracy.

Figure 11 shows the admissible parameter ranges for which one could use the simplified equations, keeping the margin of error below 50%. Also within a small range of parameters (that is,  $r_2/r_1 > 0.75$  and  $E_c/E_p > 0.01$ ), both solutions — given by Equations (16) and (19) — would yield error margins greater than 50%. Therefore, in order to obtain reliable results in the noted ranges (that is, the parameter ranges that fall within the cyan region in Figure 11), it is recommended that a FE buckling analysis be conducted.

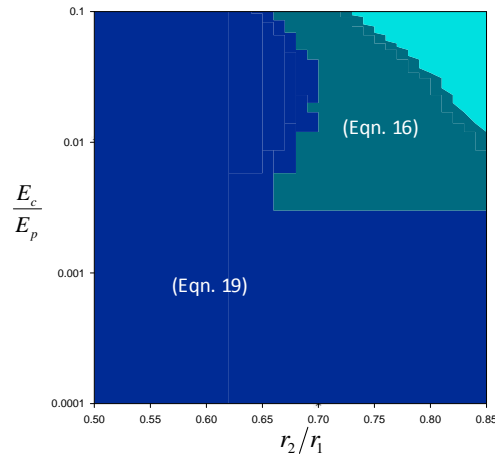


**Figure 11.** Range of parameters for which each of the simplified equations can predict the buckling pressure with less than 50% error.

## Conclusions

We used an analytical approach to develop exact and simplified (approximate) solutions for the elastic buckling pressure of sandwich pipes under external hydrostatic pressure. The parameters required to describe the characteristic equation of the system were discussed in detail. The integrity of the approximate solution given in [Brush and Almroth 1975; Sato and Patel 2007] was compared with that of this study. The practical and admissible ranges for physical and material parameters were established. The results were compared with those obtained through an extensive series of FE parametric case studies and the accuracy of the equations was assessed. Here is a summary of our conclusions:

- The contact mechanism between the core layer and the inner and outer pipes significantly affects the buckling capacity of the system.
- While for a single pipe the first buckling mode shape always corresponds to the second eigenmode (the first eigenmode would correspond to the rigid-body mode), the same does not always hold in the case of a sandwich pipe. Therefore, to find the buckling capacity of a sandwich pipe, one should explore the higher eigenmodes.
- The results obtained from the exact solution were used to validate the assumptions made in developing the simplified solution and to establish the range of applicability of the simplified solution.
- Comparison of the results obtained from the simplified solutions for the fully bonded system with those obtained from either the FE or exact analytical solutions indicated that the approximate solutions could produce reasonable accuracy for predicting the buckling capacity of the system, but for a limited range of the investigated parameters. It was shown that for stiffer core materials and greater ratios of inner to outer pipe radii, the simplified solution of [Sato and Patel 2007] would yield more accurate results. However, for the other ranges, which would fall within a more practical domain for SPs with plastic core materials, the simplified solution presented in this study would predict the buckling capacity with a higher accuracy.

- The choice from among the simplified solutions is facilitated by the graphs produced in this study. These graphs can be used to gain a sense as to what error margin one could expect when using the proposed simplified equation within a practical range.
- The comparison of the results produced by the FE analyses and those obtained from the simplified solutions for the case where the core layer could slide on the external pipe demonstrated that the simplified equation (the ATS) would produce large error margins within certain ranges; however, the solution would generate acceptable accuracy for SP systems with conventionally used core materials.

### Appendix: Coefficients of the core material stiffness matrix $K_c$

We set  $K_c = \frac{1}{\psi} LA$ , where  $L$  is given by

$$L = \begin{bmatrix} 1 & 0 & 0 & 0 \\ -nt_1/2r_1 & 1 - t_1/2r_1 & 0 & 0 \\ 0 & 0 & 1 & 0 \\ 0 & 0 & nt_2/2r_2 & 1 + t_2/2r_2 \end{bmatrix}$$

and  $\psi$  and the coefficients  $A_{ij}$  of  $A$  (for  $0 \leq i, j \leq 4$ ) are given in terms of  $R = \frac{a_2}{a_1}$  and  $\Lambda = 4\nu_c - 3$  by case-dependent formulas:

**Case I: core is fully bonded to inner and outer pipes** (nonvanishing entries only).

$$\psi = (7 + \Lambda) \{ \Lambda^2(1 + R^{4n}) - R^{2n-2}[(n^2 - 1)(R^2 - 1)^2 + (1 + R^4)\Lambda^2] \}$$

$$A_{11} = 2E_c \{ \Lambda[n(\Lambda - 1) - \Lambda - 1] - R^{4n}\Lambda[n(\Lambda - 1) + \Lambda + 1] \\ + 2R^{2n-2}[2(\Lambda - 1) + n^2(R^2 - 1)(R^2 + \Lambda - 2) + R^2(3 - \Lambda) + R^4(\Lambda^2 - 1)] \}$$

$$A_{33} = 2E_c \{ \Lambda[n(\Lambda - 1) + \Lambda + 1] - R^{4n}\Lambda[n(\Lambda - 1) - \Lambda - 1] \\ + 2R^{2n-2}[1 - \Lambda^2 + n^2(R^2 - 1)(1 + R^2(\Lambda - 2)) + R^2(\Lambda - 3) - 2R^4(\Lambda - 1)] \}$$

$$A_{22} = 2E_c \{ \Lambda[n(\Lambda - 1) - \Lambda - 1] - R^{4n}\Lambda[\Lambda + 1 + n(\Lambda - 1)] + 2R^{2n-2}[n^2\Lambda - (n^2 - 1)R^2(1 + \Lambda) + R^4(n^2 - 1 + \Lambda^2)] \}$$

$$A_{44} = 2E_c \{ \Lambda[n(\Lambda - 1) + \Lambda + 1] + R^{4n}\Lambda[\Lambda + 1 - n(\Lambda - 1)] - 2R^{2n-2}[(1 + \Lambda)(R^2 - 1 + \Lambda) + n^2(R^2 - 1)(R^2\Lambda - 1)] \}$$

$$A_{12} = A_{21} = -2E_c \{ \Lambda[1 + n + (n - 1)\Lambda] + R^{4n-2}\Lambda(n(1 + \Lambda) + \Lambda - 1) - 2nR^{2n-2}[(n^2 - 1)(R^2 - 1)^2 + R^4\Lambda^2 + \Lambda] \}$$

$$A_{34} = A_{43} = 2E_c \{ R^{4n}\Lambda[1 + n + (n - 1)\Lambda] + \Lambda(n(1 + \Lambda) + \Lambda - 1) - 2nR^{2n-2}[(n^2 - 1)(R^2 - 1)^2 + R^4\Lambda + \Lambda^2] \}$$

$$A_{13} = A_{31} = -2E_c(\Lambda - 1) \{ R^{3n-1}[(n^2 - 1)(R^2 - 1) - (1 + n + (n - 1)R^2)\Lambda] \\ + R^{n-1}[(1 + n)R^2 + n - 1)\Lambda + (n^2 - 1)(R^2 - 1)] \}$$

$$A_{14} = A_{41} = -2E_c(\Lambda - 1) \{ R^{3n-1}[(n^2 - 1)(R^2 - 1) - (1 + n - (n - 1)R^2)\Lambda] \\ + R^{n-1}[(1 + n)R^2 - n + 1)\Lambda - (n^2 - 1)(R^2 - 1)] \}$$

$$A_{23} = A_{32} = -2E_c(\Lambda - 1) \{ -R^{3n-1}[(n^2 - 1)(R^2 - 1) + (1 + n + R^2 - nR^2)\Lambda] \\ + R^{n-1}[(n^2 - 1)(R^2 - 1) + (1 + R^2 + n(R^2 - 1))\Lambda] \}$$

**Case II: Core can slide against outer pipe but is bonded to inner pipe** (nonvanishing entries only).

$$\psi = (7 + \Lambda) \{ \Lambda[n(\Lambda - 1) - 1 - \Lambda] - R^{4n}\Lambda[1 + \Lambda + n(\Lambda - 1)] + 2R^{2n-2}[n^2\Lambda - (n^2 - 1)R^2(1 + \Lambda) + R^4(n^2 - 1 + \Lambda^2)] \}$$

$$\begin{aligned}
A_{11} &= 8E_c(n^2-1)\{-\Lambda - R^{4n}\Lambda + R^{2n-2}[2R^2+n^2(R^2-1)^2+R^4(\Lambda^2-1)]\} \\
A_{13} &= A_{31} = 4E_c(n^2-1)(\Lambda-1)\{R^{3n-1}[n(R^2-1)+R^2(1-\Lambda)]+R^{n-1}[R^2(1-\Lambda)+n(1-R^2)]\} \\
A_{14} &= A_{41} = 4E_c(n^2-1)(\Lambda-1)\{R^{n-1}[n(R^2-1)-R^2(1+\Lambda)]+R^{3n-1}[R^2(1+\Lambda)-n(1-R^2)]\} \\
A_{33} &= 2E_c\{-2R^{2n-2}[2R^4(2-2\Lambda+n^2(\Lambda-2))-2n^2\Lambda-(n^2-1)R^2(\Lambda-3)(1+\Lambda)] \\
&\quad +[n^2(\Lambda-1)^2-(1+\Lambda)^2]+R^{4n}[n^2(\Lambda-1)^2-(1+\Lambda)^2]\} \\
A_{34} &= A_{34} = 2E_c\{-R^{4n}[\Lambda+1+n(\Lambda-1)][1-\Lambda+n(1+\Lambda)] \\
&\quad +[n(\Lambda-1)-\Lambda-1][\Lambda-1+n(1+\Lambda)]+4nR^{2n-2}[n^2\Lambda-(n^2-1)R^2(1+\Lambda)+R^4(n^2\Lambda-1)]\} \\
A_{44} &= 2E_c\{[n^2(\Lambda-1)^2-(1+\Lambda)^2]+R^{4n}[n^2(\Lambda-1)^2-(1+\Lambda)^2]+2R^{2n-2}[2n^2\Lambda(1+R^4)-(n^2-1)R^2(1+\Lambda)^2]\}
\end{aligned}$$

**Case III: Core can slide against inner pipe but is bonded to outer pipe** (nonvanishing entries only).

$$\begin{aligned}
\psi &= (7+\Lambda)\{\Lambda[1+\Lambda+n(\Lambda-1)]-R^{4n}\Lambda[n(\Lambda-1)-1-\Lambda]-2R^{2n-2}[(1+\Lambda)(R^2-1+\Lambda)+n^2(R^2-1)(R^2\Lambda-1)]\} \\
A_{11} &= 2E_c\{[n^2(\Lambda-1)^2-(1+\Lambda)^2]+R^{4n}[n^2(\Lambda-1)^2-(1+\Lambda)^2] \\
&\quad +2R^{2n-2}[4(\Lambda-1)-R^2(\Lambda-3)(1+\Lambda)+n^2(4-2\Lambda+2R^4\Lambda+R^2(\Lambda-3)(1+\Lambda))]\} \\
A_{21} &= A_{12} = -2E_c\{a_1^{4n}R^2[1+n(\Lambda-1)+\Lambda][1+n+(n-1)\Lambda]-R^2(a_1R)^{4n}[n(\Lambda-1)-\Lambda-1] \\
&\quad [n-1+\Lambda+n\Lambda]-4a_1^{2n}n(a_1R)^{2n}[\Lambda-1+R^2(1+\Lambda)+n^2(R^2-1)(R^2\Lambda-1)]\} \\
A_{31} &= A_{13} = -4a_1^n E_c(n^2-1)(\Lambda-1)\{R^{3n-1}(\Lambda-1+n(1-R^2))+R^{n-1}[\Lambda-1+n(R^2-1)]\} \\
A_{22} &= 2E_c\{[n^2(\Lambda-1)^2-(1+\Lambda)^2]+R^{4n}[n^2(\Lambda-1)^2-(1+\Lambda)^2]+2R^{2n-2}[2n^2\Lambda+2n^2R^4\Lambda-(n^2-1)R^2(1+\Lambda)^2]\} \\
A_{32} &= A_{23} = -4E_c(n^2-1)(\Lambda-1)\{R^{n-1}[n(R^2-1)-1-\Lambda]+R^{3n-1}[1+\Lambda+n(R^2-1)]\} \\
A_{33} &= 8E_c(n^2-1)\{\Lambda(-2-R^{4n})+R^{2n-2}[n^2(R^2-1)^2+\Lambda^2-1+2R^2]\}
\end{aligned}$$

**Case IV: Core can slide against both inner and outer pipes** (nonvanishing entries only).

$$\begin{aligned}
\psi &= (7+\Lambda)\{[n^2(\Lambda-1)^2-(1+\Lambda)^2]+R^{4n}[n^2(\Lambda-1)^2-(1+\Lambda)^2]+2R^{2n-2}[2n^2\Lambda(1+R^4)-(n^2-1)R^2(1+\Lambda)^2]\} \\
A_{11} &= -8E_c(n^2-1)\{-R^{4n}[n(\Lambda-1)-1-\Lambda]+[1+\Lambda+n(\Lambda-1)]-2R^{2n-2}[R^2(1+\Lambda)+n^2(R^2-1)(R^2\Lambda-1)]\} \\
A_{31} &= A_{13} = -8E_c(n^2-1)(\Lambda-1)\{R^{n-1}[(n-1)R^2-1-n]+R^{3n-1}[1+R^2+n(R^2-1)]\} \\
A_{33} &= -8E_c(n^2-1)\{-1-\Lambda+n(\Lambda-1)]-R^{4n}[1+\Lambda+n(\Lambda-1)]+2R^{2n-2}[n^2R^4+n^2\Lambda-(n^2-1)R^2(1+\Lambda)]\}
\end{aligned}$$

### List of symbols

AST	Simplified solution developed in this study	$r_1, r_2$	Outer and inner pipe nominal radius
$E_c, E_p$	Elastic moduli of core and pipe material	SS	Simplified solution from [Brush and Almroth 1975; Sato and Patel 2007]
$h$	Constituent's thickness		
$K_c, K_p$	Stiffness matrices of core and pipe layers	$\sigma_r$	Radial stress
$n$	Buckling mode number	$t_1, t_2$	Outer and inner pipe wall thickness
$\nu_c, \nu_p$	Poisson ratios of core and pipe material	$\tau_{r\theta}$	Tangential stress
$P$	External pressure	$v$	Tangential deformation
$P_{cr}$	Sandwich pipe buckling pressure	$w$	Radial deformation
$P_{crs}$	External pipe buckling pressure	$\phi$	Stress function

## References

- [API 2000] *API spec 5L: specification for line pipe*, 42nd ed., American Petroleum Institute, Washington, DC, 2000.
- [Brush and Almroth 1975] D. O. Brush and B. Almroth, *Buckling of bars, plates and shells*, McGraw-Hill, New York, 1975.
- [Castello and Estefen 2006] X. Castello and S. F. Estefen, “Adhesion effect on the ultimate strength of sandwich pipes”, in *Proceedings of the 25th International Conference on Offshore Mechanics and Arctic Engineering* (Hamburg, 2006), ASME, New York, 2006. Paper OMAE2006-92481.
- [Castello and Estefen 2007] X. Castello and S. F. Estefen, “Limit strength and reeling effects of sandwich pipes with bonded layers”, *Int. J. Mech. Sci.* **49**:5 (2007), 577–588.
- [Castello and Estefen 2008] X. Castello and S. F. Estefen, “Sandwich pipes for ultra deepwater applications”, in *Offshore Technology Conference, OTC 08: Waves of change* (Houston, 2008), Curran Associates, Redhook, NY, 2008. Paper 19704-MS.
- [Castello et al. 2009] X. Castello, S. F. Estefen, H. R. Leon, L. C. Chad, and J. Souza, “Design aspects and benefits of sandwich pipes for ultra deepwaters”, in *Proceedings of the 28th International Conference on Ocean, Offshore and Arctic Engineering* (Honolulu, HI, 2009), ASME, New York, 2009. Paper OMAE2009-79528.
- [Estefen et al. 2005] S. F. Estefen, T. A. Netto, and I. P. Pasqualino, “Strength analyses of sandwich pipes for ultra deepwaters”, *J. Appl. Mech. (ASME)* **72**:4 (2005), 599–608.
- [Farshad 1994] M. Farshad, *Stability of structures*, Elsevier, Amsterdam, 1994.
- [Kardomateas and Simitse 2002] G. A. Kardomateas and G. J. Simitse, “Buckling of long, sandwich cylindrical shells under pressure”, pp. 327–328 in *Proceedings of the 6th International Conference on Computational Structures Technology* (Prague, 2002), edited by B. H. V. Topping and Z. Bittnar, Civil-Comp Press, Stirlingshire, 2002. Paper 140.
- [Kardomateas and Simitse 2005] G. A. Kardomateas and G. J. Simitse, “Buckling of long sandwich cylindrical shells under external pressure”, *J. Appl. Mech. (ASME)* **72**:4 (2005), 493–499.
- [Kyriakides 2002] S. Kyriakides, “Buckle propagation in pipe-in-pipe systems, I: Experiments”, *Int. J. Solids Struct.* **39**:2 (2002), 351–366.
- [Kyriakides and Corona 2007] S. Kyriakides and E. Corona, *Mechanics of offshore pipelines*, Elsevier, Amsterdam, 2007.
- [Kyriakides and Netto 2002] S. Kyriakides and T. A. Netto, “Dynamic propagation and arrest of buckles in pipe-in-pipe systems”, pp. 199–205 in *Proceedings of the 21st International Conference on Offshore Mechanics and Arctic Engineering* (Oslo, 2002), vol. 4, edited by T. Jones et al., ASME, New York, 2002. Paper OMAE2002-28600.
- [Kyriakides and Netto 2004] S. Kyriakides and T. A. Netto, “On the dynamic propagation and arrest of buckles in pipe-in-pipe systems”, *Int. J. Solids Struct.* **41**:20 (2004), 5463–5482.
- [Kyriakides and Vogler 2002] S. Kyriakides and T. J. Vogler, “Buckle propagation in pipe-in-pipe systems, II: Analysis”, *Int. J. Solids Struct.* **39**:2 (2002), 367–392.
- [Ohga et al. 2005] M. Ohga, A. Sanjeeva Wijenayaka, and J. G. A. Croll, “Reduced stiffness buckling of sandwich cylindrical shells under uniform external pressure”, *Thin-Walled Struct.* **43**:8 (2005), 1188–1201.
- [Sato and Patel 2007] M. Sato and M. H. Patel, “Exact and simplified estimations for elastic buckling pressures of structural pipe-in-pipe cross sections under external hydrostatic pressure”, *J. Mar. Sci. Technol.* **12**:4 (2007), 251–262.
- [Sato et al. 2008] M. Sato, M. H. Patel, and F. Trarieux, “Static displacement and elastic buckling characteristics of structural pipe-in-pipe cross-sections”, *Struct. Eng. Mech.* **30**:3 (2008), 263–278.
- [Timoshenko and Goodier 1970] S. Timoshenko and J. N. Goodier, *Theory of elasticity*, 3rd ed., McGraw-Hill, New York, 1970.

Received 9 Jun 2009. Revised 21 Oct 2009. Accepted 30 Oct 2009.

Department of Civil and Resource Engineering, Dalhousie University

KAVEH ARJOMANDI: [kaveh.arjomandi@dal.ca](mailto:kaveh.arjomandi@dal.ca)

Dalhousie University, Department of Civil and Resource Engineering, 1360 Barrington Street, Halifax, NS B3J 1Z1, Canada

FARID TAHERI: [farid.taheri@dal.ca](mailto:farid.taheri@dal.ca)

Dalhousie University, Department of Civil and Resource Engineering, 1360 Barrington Street, Halifax, NS B3J 1Z1, Canada

# JOURNAL OF MECHANICS OF MATERIALS AND STRUCTURES

<http://www.jomms.org>

Founded by Charles R. Steele and Marie-Louise Steele

## EDITORS

CHARLES R. STEELE Stanford University, U.S.A.  
DAVIDE BIGONI University of Trento, Italy  
IWONA JASIUK University of Illinois at Urbana-Champaign, U.S.A.  
YASUhide SHINDO Tohoku University, Japan

## EDITORIAL BOARD

H. D. BUI École Polytechnique, France  
J. P. CARTER University of Sydney, Australia  
R. M. CHRISTENSEN Stanford University, U.S.A.  
G. M. L. GLADWELL University of Waterloo, Canada  
D. H. HODGES Georgia Institute of Technology, U.S.A.  
J. HUTCHINSON Harvard University, U.S.A.  
C. HWU National Cheng Kung University, R.O. China  
B. L. KARIHALOO University of Wales, U.K.  
Y. Y. KIM Seoul National University, Republic of Korea  
Z. MROZ Academy of Science, Poland  
D. PAMPLONA Universidade Católica do Rio de Janeiro, Brazil  
M. B. RUBIN Technion, Haifa, Israel  
A. N. SHUPIKOV Ukrainian Academy of Sciences, Ukraine  
T. TARNAI University Budapest, Hungary  
F. Y. M. WAN University of California, Irvine, U.S.A.  
P. WRIGGERS Universität Hannover, Germany  
W. YANG Tsinghua University, P.R. China  
F. ZIEGLER Technische Universität Wien, Austria

## PRODUCTION

PAULO NEY DE SOUZA Production Manager  
SHEILA NEWBERY Senior Production Editor  
SILVIO LEVY Scientific Editor

Cover design: Alex Scorpan

See inside back cover or <http://www.jomms.org> for submission guidelines.

JoMMS (ISSN 1559-3959) is published in 10 issues a year. The subscription price for 2010 is US \$/year for the electronic version, and \$/year (+\$ shipping outside the US) for print and electronic. Subscriptions, requests for back issues, and changes of address should be sent to Mathematical Sciences Publishers, Department of Mathematics, University of California, Berkeley, CA 94720-3840.

JoMMS peer-review and production is managed by EditFlow™ from Mathematical Sciences Publishers.

PUBLISHED BY

 **mathematical sciences publishers**  
<http://www.mathscipub.org>

A NON-PROFIT CORPORATION

Typeset in L<sup>A</sup>T<sub>E</sub>X

©Copyright 2010. Journal of Mechanics of Materials and Structures. All rights reserved.

<b>Chaotic vibrations in a damage oscillator with crack closure effect</b> NOËL CHALLAMEL and GILLES PIJAUDIER-CABOT	<b>369</b>
<b>Elastic buckling capacity of bonded and unbonded sandwich pipes under external hydrostatic pressure</b> KAVEH ARJOMANDI and FARID TAHERI	<b>391</b>
<b>Elastic analysis of closed-form solutions for adhesive stresses in bonded single-strap butt joints</b> GANG LI	<b>409</b>
<b>Theoretical and experimental studies of beam bimorph piezoelectric power harvesters</b> SHUDONG YU, SIYUAN HE and WEN LI	<b>427</b>
<b>Shakedown working limits for circular shafts and helical springs subjected to fluctuating dynamic loads</b> PHAM DUC CHINH	<b>447</b>
<b>Wave propagation in carbon nanotubes: nonlocal elasticity-induced stiffness and velocity enhancement effects</b> C. W. LIM and Y. YANG	<b>459</b>
<b>Dynamic compressive response of composite corrugated cores</b> BENJAMIN P. RUSSELL, ADAM MALCOM, HAYDN N. G. WADLEY and VIKRAM S. DESHPANDE	<b>477</b>
<b>Effects of surface deformation on the collective buckling of an array of rigid beams on an elastic substrate</b> HAOJING LIN, ZIGUANG CHEN, JIASHI YANG and LI TAN	<b>495</b>
<b>Improved hybrid elements for structural analysis</b> C. S. JOG	<b>507</b>